DOI https://doi.org/10.32782/1994-4691-2026-1-77-8
UDK 621.22

CONTROL MODES OF A HYDRAULIC DRIVE WITH INDEPENDENT CONTROL OF FLOWS UNDER DIFFERENT LOAD CONDITIONS

РЕЖИМИ КЕРУВАННЯ В ГІДРОПРИВОДІ З НЕЗАЛЕЖНИМ КЕРУВАННЯМ ПОТОКАМИ ПРИ РІЗНИХ УМОВАХ НАВАНТАЖЕННЯ

O. A. Syrotin[1], graduate student ORCID: 0009-0002-4992-3845
D. O. Lozinskyi[1*], Ph.D., Associate Professor ORCID: 0000-0002-1077-1621

[1] *Vinnytsia National Technical University, Vinnytsia, Ukraine*
* e-mail: lozinskiy_dmitriy@vntu.edu.ua

Abstract. A hydraulic drive of a mobile machine under a passive load is considered, based on proportional metering elements that independently control the inlet and outlet flows of the hydraulic cylinder and on controlled check valves. The influence of the load mass, the load force direction and the required rod velocity on the choice of the control mode is studied. Four modes are analysed: meter-in control, meter-out control with pump unloading, combined control and control by the pump flow rate. A quasi-static model with constraints on cavitation, pressure, flow rate and controllability is compiled; the comparison criterion is the total pressure drop across the metering elements. A mode map in the coordinates “load mass – required velocity” is built and the energy consumed from the pump over a loader cycle is analysed.

Keywords: proportional metering element, controlled check valve, quasi-static model, total pressure drop, cavitation, front loader, pump unloading, energy efficiency.

Introduction.

Hydraulic drives of mobile machines used for loading and unloading operations work under a passive load for a considerable part of their operating time; the sign of this load with respect to the velocity of the working element changes during the cycle, while its magnitude is determined by the load mass and the position of the links. The hydraulic drives of such machines usually employ directional control valves in which the flows at the inlet and outlet of the hydraulic motor are controlled by a common spool, so the ratio of the flow areas of the inlet and outlet passages is fixed by the spool geometry and cannot be changed according to the load conditions. Metering elements with independent flow control (independent metering) [1, 2] do not have this limitation: the opening of each metering element can be set separately, while controlled check valves ensure the sealing of the working chambers of the hydraulic cylinder. However, such a structure is more complex and, in order to realise its advantages, requires the choice of a rational control mode for every combination of operating conditions.

The boom circuit of the PKU-0.8 front loader mounted on the MTZ-82 tractor (Fig. 1) is taken for the study. The boom OB rotates about the pivot O on the frame, the hydraulic cylinder CD rests on the frame at point C and acts on the boom at point D, and the load of mass *m* is applied at point B. The mass on the boom varies from the mass of the empty bucket to the rated one, i.e. approximately six times, and the sign of the load force with respect to the rod velocity changes twice per cycle. With coupled meter-in/meter-out control, the overrunning load during lowering is controlled by the outlet passage, whereas the inlet passage of the same spool throttles the pump flow without any functional need, the pump remains under pressure in all phases of motion, and the energy dissipated across the metering elements is converted into heat and causes heating of the working fluid.

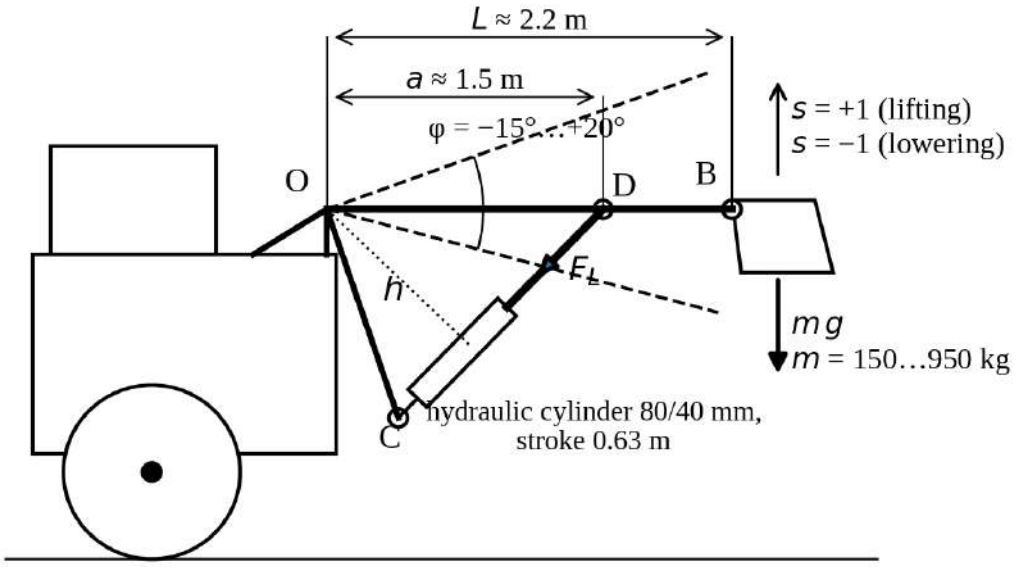


Fig. 1. Kinematic diagram of the boom circuit of the PKU-0.8 loader: O – boom pivot on the frame; C, D – hydraulic cylinder pivots; B – point of load application; *L*, *a* – link lengths; *h* – lever arm of the cylinder force about O (in the middle position *h* ≈ 1.08 m); φ – boom rotation angle; F_L – force on the rod; *s* – sign of the force direction with respect to the velocity. The dimensions are estimates and are to be refined according to the machine data sheet

At a small mass, the pressure produced by the load in the piston-side chamber is insufficient to pass the required flow rate through the outlet passage, which limits the lowering velocity. Independent flow control removes the structural coupling of the passages but gives rise to the problem of choosing the control mode for every combination of mass, sign of the force and required velocity. In the absence of appropriate recommendations, or when irrational control modes are applied, the advantages of independent control are not realized or are realised only partially, and an erroneous choice of the mode under an overrunning load may lead to cavitation and uncontrolled motion.

Literature Review.

Independent control of the inlet and outlet of a hydraulic cylinder as a means of reducing throttling losses and of solving the overrunning-load problem was proposed in [3]. The authors of [4, 5] identified five control modes for a four-valve hydraulic unit and formulated the mode-switching problem according to an energy criterion in a quasi-static formulation; in their work, meter-out control with subsequent regeneration is preferable under an overrunning load. In [6] a method of controlling four valves with cavitation prevention was proposed, and in the patent [7] the control mode is selected according to the sign and magnitude of the load pressure and the required velocity.

The authors of [8] systematised the structures of independent-metering systems and their problems, in particular the loss of controllability at small pressure drops and shocks during switching. In [9] the operating modes of “programmable valves” were selected according to an energy criterion.

In [10–13] the coordination of the pump and the valves [10], bumpless mode switching [11], the reduction of oscillations during switching [12] and switching between flow and pressure control [13] were investigated. The state of the field is summarised in the reviews [14, 15], and a separate review is devoted to the coordinated control of the inlet and outlet under a sustained overrunning load [16]. The architectures of independent-metering systems and their operating modes are summarised in [17–19], trends in the control of multi-actuator

hydraulic systems of mobile machines in [20, 21], and the effect of such systems on the energy consumption of excavators is investigated in [22–24].

The author of [25] substantiated the application of adaptive control systems for the hydraulic drives of manipulators of mobile machines. In [1, 2] a proportional directional control valve with independent flow control was developed and optimised, and in [26] a multi-mode hydraulic drive of a front loader was investigated. In previous works of the authors, approaches to improving the energy efficiency of electrohydraulic systems [27], a test bench for studies under a passive load [28], the influence of the control system parameters on the drive dynamics and the energy performance of throttling, load-sensing and displacement control over a duty cycle were considered [29].

At the same time, for a two-spool valve without regenerative connections, the regions of applicability of the control modes under a passive load in the coordinates “mass – force direction — velocity” have not been quantified. The available selection rules were obtained for four-valve units with regeneration or are formulated in general terms.

Research Methodology.

The aim of the work is to investigate different control modes of a hydraulic drive with a passive load according to the criterion of minimising the total pressure drop across the metering elements and reducing the energy consumption. To achieve this aim, the following tasks have to be solved: 1) to substantiate the design scheme of the hydraulic drive and to identify the flow control modes; 2) to build a quasi-static mathematical model of the steady state with constraints on cavitation, pressure, flow rate and controllability; 3) to calculate the pressures, pressure drops, power and efficiency for a grid of conditions “mass — force direction — velocity” and to identify inadmissible combinations; 4) to build a mode map for resistive and overrunning loads; 5) to analyse the energy effect of mode switching on a conventional duty cycle of the loader.

The hydraulic circuit diagram of the drive is shown in Fig. 2.

The pump 1 feeds the pressure line; the metering section 2 contains the proportional two-position metering elements 5 of lines A and B, each of which in the rest position (under the spring action) connects its line to the return line through a throttling orifice and in the working position – to the pressure line. The intermediate position of the spool of the proportional element sets the flow area A_1 (line A) or A_2 (line B). The load-holding section 3 contains the controlled check valves 6, which in the rest position pass the flow only towards the working chamber (load holding and make-up of the chamber from the return line) and, when energised, open a free passage in both directions. The shuttle valve 7 transmits the higher of the pressures of lines A and B to the bypass compensator 8 – the pump flow control element, which discharges the surplus pump flow to the return line and maintains the pressure in the pressure line at a level exceeding the load pressure by a constant margin. During load holding and during motion under the action of the load, the compensator is fully open and the pump pressure falls to P_{unl}. The pressure relief valve 9 limits the pressure in the pressure line. The hydraulic cylinder 4 has a piston-side chamber of area F_1 (pressure P_1) and a rod-side chamber of area F_2 (pressure P_2); the load force F_{L} acts on the rod, and the rod moves with velocity v. The design of the metering elements is considered in [1, 2].

Hereinafter the subscripts “in” and “out” denote the role of the working chamber and of the metering element: “in” – the chamber being filled and the element through which the flow enters it, “out” – the chamber being emptied and the element through which the flow goes to the return line. The sign $s = +1$ corresponds to a resistive load (the force is directed against the rod velocity, lifting of the load), $s = -1$ – to an overrunning load (lowering of the load). At $s = +1$, $P_{\text{in}} = P_1$, $F_{\text{in}} = F_1$, $A_{\text{in}} = A_1$, $P_{\text{out}} = P_2$, $F_{\text{out}} = F_2$, $A_{\text{out}} = A_2$; at $s = -1$ the roles are interchanged.

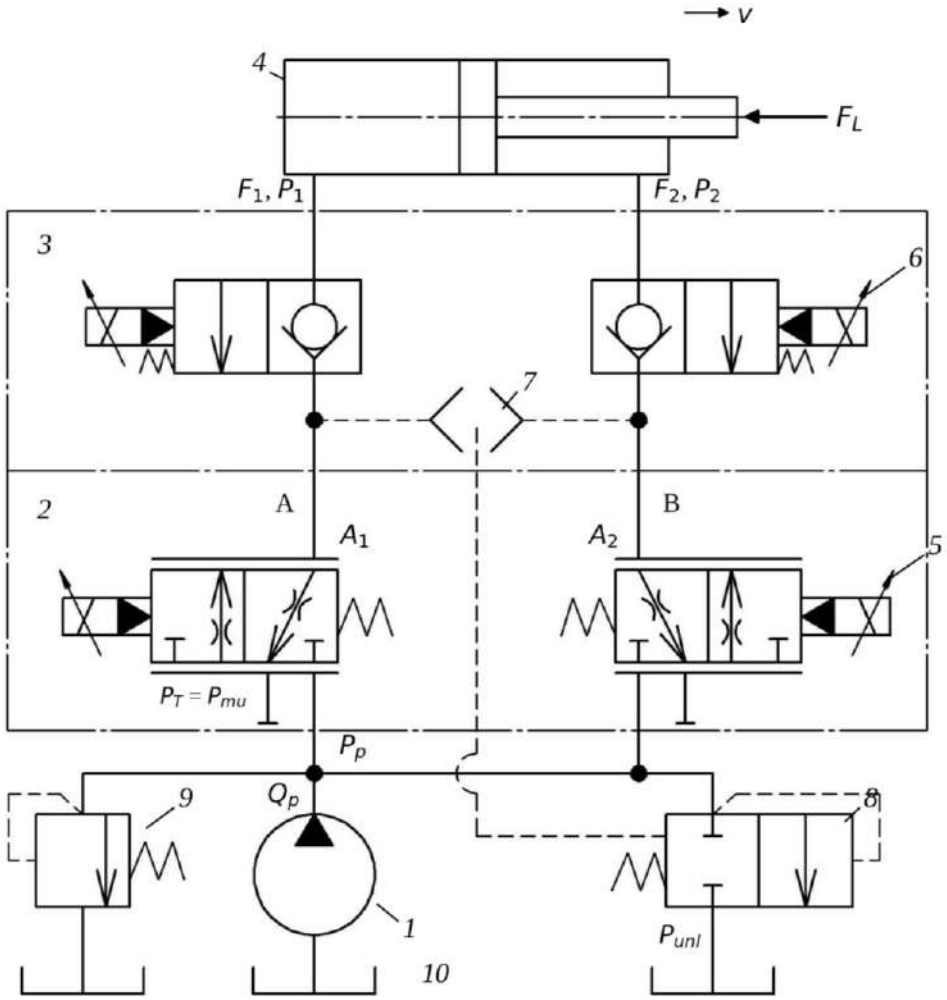


Fig. 2. Hydraulic circuit diagram of the drive with independent flow control: 1 – pump; 2 – metering section; 3 – load-holding section; 4 – hydraulic cylinder; 5 – proportional two-position metering elements of lines A and B (flow areas A_1, A_2); 6 – controlled check valves; 7 – shuttle valve; 8 – bypass compensator (pump flow control element); 9 – pressure relief valve; 10 – tank. P_p, Q_p – pump pressure and flow rate; P_T, P_{mu} – return-line and make-up pressures; P_{unl} – pressure of the unloaded pump; P_1, P_2, F_1, F_2 – pressures and areas of the working chambers; F_L – load force; v – rod velocity

Four flow control modes are distinguished for this circuit (Table 1). In mode M1 the velocity is set by the meter-in element while the meter-out element is fully open, which is the conventional variant for a resistive load. In mode M2 the flow is controlled by the meter-out element while the meter-in element is fully open; under an overrunning load the inlet chamber is filled by the make-up flow from the return line and the pump is unloaded. Mode M3, in which both elements are partially closed, is intended for intermediate cases where M1 may cause cavitation and M2 does not provide controllability. In mode M4 both elements are open and the velocity is set by the supply flow rate (displacement or rotational speed of the pump); this mode is the limiting one and is equivalent to displacement control [30].

A quasi-static model of steady motion is used to compare the modes. The choice is due to three circumstances. First, the mode selection rule is formulated for conditions that change slowly in comparison with the transient processes: the phases of the loader duty cycle last for seconds, whereas the transients in the drive last for fractions of a second [29], and the energy balance of a phase is determined by the steady values of pressures and flow rates. Second, the constraints that determine the admissibility of a mode (cavitation, admissible pressure, flow rate, controllability) are formulated for the steady state. Third, the dynamics of switching between the modes is a separate problem which will be considered at the next stage.

Table 1. State of the drive elements in the flow control modes

Mode	Meter-in element A_{in}	Meter-out element A_{out}	Power source (pump)
M1	controls the flow	fully open	under pressure
M2	fully open (at $s = -1$ – line on make-up)	controls the flow	under pressure (at $s = -1$ – unloaded)
M3	controls the flow	controls the flow	under pressure
M4	fully open	fully open	controlled flow rate

The following assumptions are adopted: 1) the working fluid is incompressible, its density and temperature are constant, wave processes in the hydraulic lines are not considered; 2) the rod velocity is constant, inertia forces and viscous damping forces are neglected; 3) leakages in the metering elements and in the hydraulic cylinder as well as pressure losses in the hydraulic lines are neglected; 4) the friction force in the hydraulic cylinder is proportional to the load force; 5) the flow rate through a metering element is described by a quadratic dependence on the pressure drop with a constant discharge coefficient; 6) the power source is a fixed-displacement pump with a bypass compensator that maintains the pressure in the pressure line at the minimum necessary level and discharges the surplus flow to the return line at this pressure (a load-sensing scheme with a fixed-displacement pump according to [30]); losses in the pump itself are not considered; 7) the make-up of a working chamber from the return line through the throttling orifice of the metering element in the rest position and the check valve maintains a constant pressure in the chamber at a flow rate not exceeding the pump flow rate; 8) a metering element retains controllability if the pressure drop across it is not less than the minimum controllable one and its opening does not exceed the admissible fraction of the maximum; the metering element operates at the lowest admissible pressure drop.

For given mass m, force direction s and velocity v^*, the steady state is described by the system of equations:

$$P_{in}\cdot F_{in} - P_{out}\cdot F_{out} = s\cdot F_L + k_{fr}\cdot F_L, \quad F_L = k_r\cdot m\cdot g \tag{1}$$

$$Q_{in} = F_{in}\cdot v^*, \quad Q_{out} = F_{out}\cdot v^* \tag{2}$$

$$\Delta p_{in} = (\rho/2)\cdot(Q_{in}/(\mu\cdot A_{in}))^2, \quad \Delta p_{out} = (\rho/2)\cdot(Q_{out}/(\mu\cdot A_{out}))^2 \tag{3}$$

$$P_{out} = P_T + \Delta p_{out}; \quad P_p = P_{in} + \Delta p_{in} \text{ (M1, M3, M4; M2 at } s = +1) \tag{4}$$

$$P_{in} = P_{mu}, \quad P_p = P_{unl} \text{ (M2 at } s = -1) \tag{5}$$

$$A = A_{max} \text{ (open element)}; \quad \Delta p = \max(\Delta p_c; \Delta p(A_{max})) \text{ (metering element, } s = +1) \tag{6}$$

$$P_{in}, P_{out} \ge P_{min}; \quad P_p \le P_{max}; \quad Q_{in} \le Q_p; \quad \Delta p_{met} \ge \Delta p_c; \quad A_{met} \le k_A\cdot A_{max} \tag{7}$$

$$\Sigma\Delta p = \Delta p_{in} + \Delta p_{out}; \quad N_d = \Delta p_{in}\cdot Q_{in} + \Delta p_{out}\cdot Q_{out} \tag{8}$$

$$N_p = P_p\cdot Q_p \text{ (M1–M3)}, \quad N_p = P_p\cdot Q_{in} \text{ (M4)}; \quad \eta = (s + k_{fr})\cdot F_L\cdot v^*/N_p, \tag{9}$$

where P_{in}, P_{out} are the pressures in the chambers being filled and emptied; F_{in}, F_{out} are their areas; F_L is the load force on the rod; k_{fr} is the friction coefficient; k_r is the coefficient of reduction of the mass to the force on the rod according to the boom kinematics (Fig. 1); g is the gravitational acceleration; Q_{in}, Q_{out} are the flow rates through the meter-in and meter-out elements; Δp_{in}, Δp_{out} are the pressure drops across them; ρ is the working fluid density; μ is the discharge coefficient; A_{in}, A_{out} are the flow areas; A_{max} is the flow area of a fully open element; P_p is the pump pressure; P_T, P_{mu}, P_{unl} are the return-line pressure, the make-up pressure and the pressure of the unloaded pump; P_{min} is the pressure below which cavitation occurs; P_{max} is the admissible pressure; Q_p is the pump flow rate (for M2 at $s = -1$ — the capacity of the make-up path); Δp_{met}, A_{met} are the pressure drop across and the flow area of the

metering element; Δp_c is the minimum controllable pressure drop; k_A is the admissible opening fraction; $\Sigma\Delta p$ is the total pressure drop across the metering elements (the comparison criterion); N_d is the power dissipated across them; N_p is the power consumed from the pump; η is the transmission efficiency from the pump to the rod (calculated at $s = +1$; during lowering there is no useful work and N_p serves as the indicator). For mode M3 at $s = -1$ a pressure not lower than the guaranteed value P_g is maintained in the inlet chamber.

The initial data of the model and the ranges of their variation are summarised in Table 2. The design example corresponds to the boom circuit of the PKU-0.8 loader: hydraulic cylinder 80/40 mm, NSh-32 gear pump. The area A_{max} is chosen so that at full opening the pressure drop is 0.3 MPa at the pump flow rate. The highest attainable lifting velocity is $Q_p/F_1 = 0.182$ m/s and the lowering velocity is $Q_p/F_2 = 0.243$ m/s; therefore a velocity of 0.3 m/s is unattainable with the NSh-32 pump in any mode and is replaced by 0.15 m/s in the calculation grid.

Table 2. Initial data of the mathematical model

Symbol	Parameter	Value / range	Unit
F_1 / F_2	areas of the piston-side and rod-side chambers (cylinder 80/40 mm)	50.3 / 37.7	cm^2
S	rod stroke	0.63	m
Q_p	flow rate of the NSh-32 pump at 1700 rpm	55	l/min
m	load mass (5 levels; continuous for the map)	150…950	kg
k_r	coefficient of reduction of the mass to the force on the rod (estimate)	2.04	—
F_L	load force on the rod	3…19	kN
k_{fr}	friction coefficient	0.03	—
s	direction of the load force	+1; −1	—
v^*	required velocity (grid; 0.02…0.30 for the map)	0.05; 0.10; 0.15	m/s
μ; ρ	discharge coefficient; working fluid density	0.65; 870	—; kg/m^3
A_{max}	flow area of a fully open element	54	mm^2
$P_{min} = P_{mu} = P_T$	cavitation, make-up and return-line pressures	0.15	MPa
P_{max}; P_{rv}	admissible pressure; relief valve setting	16; 17	MPa
Δp_c; k_A	minimum controllable pressure drop; admissible opening fraction	0.5; 0.8	MPa; —
P_g; P_{unl}	guaranteed pressure in the inlet chamber (M3); pressure of the unloaded pump	0.5; 0.3	MPa
P_{sb}	standby pressure of the supply with coupled control (cycle, strategy A)	0.5	MPa

The system of equations (1)–(9) is solved sequentially without iterations. The flow rates are determined from (2), the pressure drops across the open and metering elements from (3) and (6), P_{out} from (4), P_{in} from (1) and P_p from (4). Then the constraints (7) are checked and the indicators (8), (9) are calculated. For M2 and M3 at $s = -1$ the order is different: P_{in} is prescribed (the make-up pressure according to (5) or the guaranteed pressure), P_{out} and the

pressure drop across the meter-out element are found from (1), and its flow area is found from (3) and checked against (7). For M3 the pressure P_{in} is raised to the value at which the meter-out element satisfies (7). A mode is considered inadmissible if at least one of the constraints (7) is violated. For M1 at $s = -1$ the calculated pressure deficit in the inlet chamber and the velocity of uncontrolled motion with a fully open meter-out element are recorded. The calculation is implemented in Python (NumPy and Matplotlib libraries) for a grid of 5 × 3 × 2 × 4 = 120 combinations "mass × velocity × direction × mode" and for the mode map on a grid of 81 × 141 points in the coordinates (m, v^*). The conventional cycle is calculated with the same model phase by phase.

Results.

Under a resistive load (Fig. 3) the total pressure drop across the metering elements does not depend on the mass (Fig. 3, a): the adaptive supply raises the pressure together with the load, and the pressure drops are determined only by the flow rate and the minimum controllable pressure drop. At $v^* = 0.15$ m/s, $\Sigma\Delta p$ is 0.61 MPa for M1, 0.70 MPa for M2, 1.00 MPa for M3 and 0.32 MPa for M4. The dependence on velocity (Fig. 3, b) explains the origin of this difference: in M1 and M2 one element operates at the constant pressure drop Δp_c, while the other, open, element adds a pressure drop that grows quadratically with velocity. In M4 both elements are open, so at 0.05 m/s $\Sigma\Delta p = 0.04$ MPa against 0.51 MPa in M1, i.e. 14 times less, and at 0.15 m/s — 0.32 against 0.61 MPa, 1.9 times less.

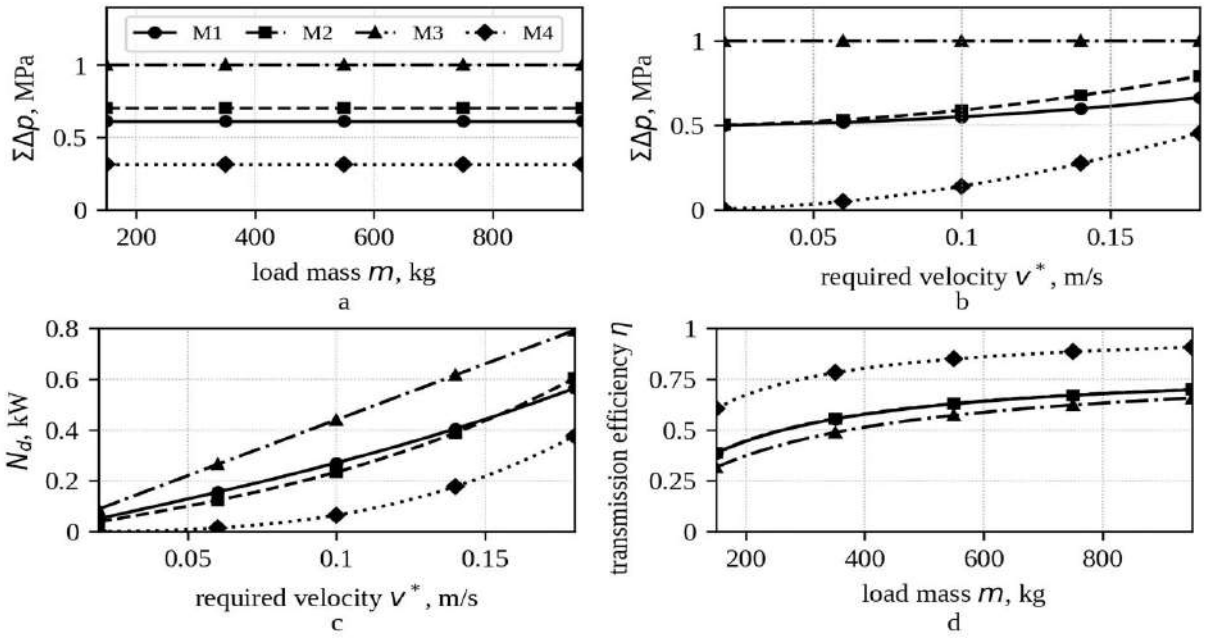


Fig. 3. Mode indicators under a resistive load (s = +1): a – total pressure drop versus mass; b – total pressure drop versus required velocity; c – power dissipated across the metering elements; d – transmission efficiency

The advantage of M1 over M2 is due to the fact that the open element in M1 passes the smaller flow rate $Q_{out} = 0.75 \cdot Q_{in}$. In terms of the power dissipated across the elements (Fig. 3, c), M1 and M2 are equivalent, because the pressure drop across the meter-out element acts on the smaller flow rate, and at low velocities M2 has a slight advantage. Mode M3 is inferior to M1 by a factor of two in $\Sigma\Delta p$ and by 6…22 % in the power consumed from the pump (Table 3); therefore, under a resistive load it can be justified only by positioning accuracy requirements, which are not analysed in the quasi-static formulation. The transmission efficiency (Fig. 3, d) increases with the mass for all modes: for M1 from 0.39 at 150 kg to 0.70 at 950 kg, for M4 from 0.61 to 0.91. The pressure constraint is not reached in the example: at 950 kg P_p does not exceed 4.9 MPa.

Under an overrunning load (Fig. 4) the relations between the indicators change. In mode M1 with a fully open meter-out element the pressure in the chamber being emptied is only 0.17…0.35 MPa, and the force balance (1) requires a negative pressure in the inlet chamber: from −0.30 MPa at 150 kg to −4.42 MPa at 950 kg (Fig. 4, b). This corresponds to a discontinuity of the flow in the inlet chamber, opening of the make-up path and uncontrolled motion with a velocity limited only by the resistance of the fully open meter-out element. According to (1), (3), at $P_{in} = P_{min}$ this velocity is 0.24 m/s at 150 kg and 0.63 m/s at 950 kg. M1 is unsuitable for an overrunning load over the whole range, which agrees with the known result for meter-in control [3, 8]. Mode M4 is also unsuitable: control by the supply flow rate does not limit the velocity under an overrunning load, since the motion is produced by the load force and not by the supply flow.

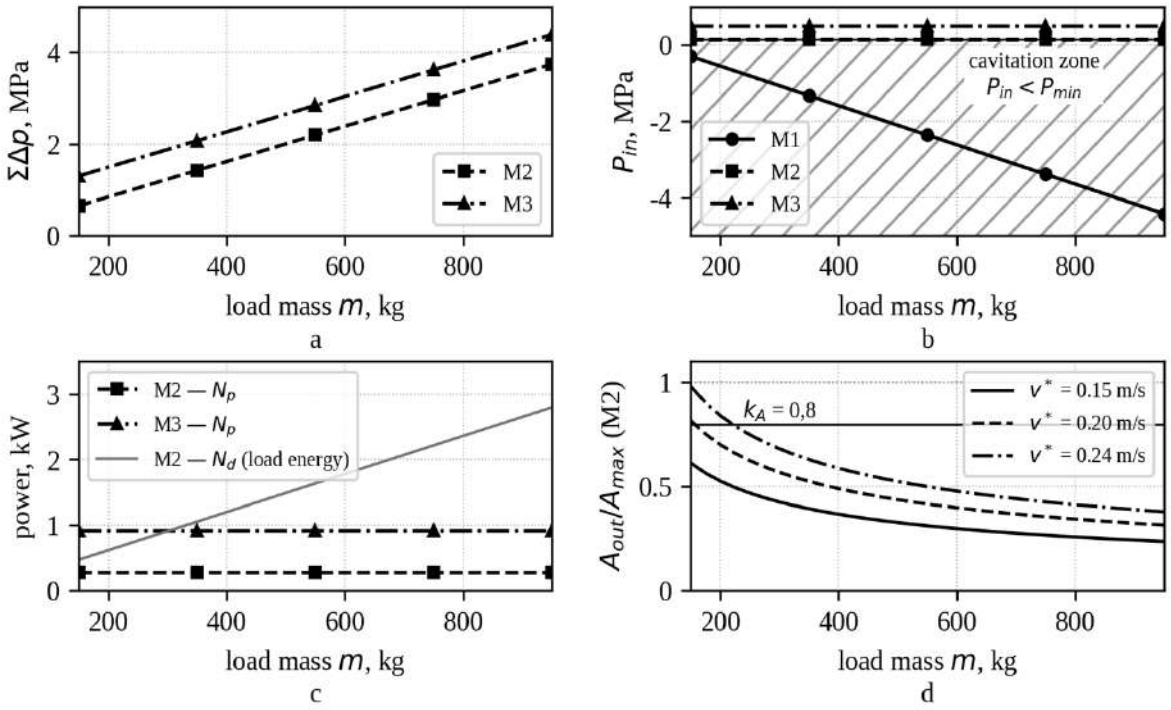


Fig. 4. Mode indicators under an overrunning load ($s = -1$), $v^* = 0.15$ m/s: a – total pressure drop; b – pressure in the inlet chamber (hatching – cavitation zone); c – power consumed from the pump N_p and power N_d dissipated across the elements in M2; d – relative opening of the meter-out element in M2 at three velocities

In mode M2 the pressure in the inlet chamber is maintained by the make-up flow, and the potential energy of the load is dissipated across the meter-out element: P_{out} = 0.69 MPa at 150 kg and 3.78 MPa at 950 kg, $\Sigma\Delta p$ = 0.66…3.74 MPa (Fig. 4, a). This pressure drop corresponds to the dissipation of the potential energy of the load (curve N_d in Fig. 4, c) and cannot be eliminated in a throttling scheme.

The energy difference between the modes consists only in whether the pump work is added to it. In M2 the pump is unloaded and consumes 0.28 kW. In mode M3 the pump produces P_{in} = 0.5 MPa in the inlet chamber, which raises P_{out} by 0.26 MPa and adds a pressure drop of 0.5 MPa across the meter-in element: $\Sigma\Delta p$ = 1.30…4.39 MPa, i.e. 2.0 times more than in M2 at 150 kg and 17 % more at 950 kg, while the power consumed from the pump increases to 0.92 kW (Fig. 4, c). M3 can be justified only by the controllability condition. Fig. 4, d shows the relative opening of the meter-out element in M2: at 0.15 m/s it does not exceed 0.6 for all masses, but at 0.20…0.24 m/s and masses up to 230 kg it exceeds the admissible value k_A = 0.8, i.e. the element is almost fully open and loses its ability to control the flow. This corresponds to the case of fast lowering of the empty bucket: the pressure produced by the bucket in the piston-side chamber is insufficient to pass the required

flow rate through the meter-out element, and an additional force from the pump pressure in the inlet chamber is needed to reach the required velocity. The results for the characteristic points are summarised in Table 3.

Table 3. Calculation results for the characteristic points, $v^* = 0.15$ m/s

Condition	Mode	P_{in}, MPa	P_{out}, MPa	P_p, MPa	$\Sigma\Delta p$, MPa	N_p, kW	η	Note
m = 950 kg, s = +1	M1	4.09	0.26	4.59	0.61	4.21	0.70	—
	M2	4.38	0.65	4.58	0.70	4.20	0.70	—
	M3	4.38	0.65	4.88	1.00	4.47	0.66	—
	M4	4.09	0.26	4.29	0.32	3.24	0.91	controllable-flow supply
m = 150 kg, s = +1	M1	0.81	0.26	1.31	0.61	1.20	0.39	—
	M2	1.10	0.65	1.31	0.70	1.20	0.39	—
	M3	1.10	0.65	1.60	1.00	1.47	0.32	—
	M4	0.81	0.26	1.02	0.32	0.77	0.61	controllable-flow supply
m = 950 kg, s = −1	M1	−4.42	0.35	—	—	—	—	cavitation, uncontrolled motion 0.63 m/s
	M2	0.15	3.78	0.30	3.74	0.28	—	pump unloaded
	M3	0.50	4.04	1.00	4.39	0.92	—	—
m = 150 kg, s = −1	M1	−0.30	0.35	—	—	—	—	cavitation, uncontrolled motion 0.24 m/s
	M2	0.15	0.69	0.30	0.66	0.28	—	pump unloaded
	M3	0.50	0.95	1.00	1.30	0.92	—	—

* Note. M4 at s = −1 is unsuitable: the supply flow does not restrain an overrunning load.

The effect of mode switching is analysed on a conventional cycle of a loader with a bucket: lifting of a 950 kg load over the full stroke at a velocity of 0.15 m/s (4.2 s), holding during transport (10 s), lowering of the empty 150 kg bucket at the same velocity (4.2 s) and holding of the empty bucket (6 s). Strategy A reproduces a conventional spool valve with coupled meter-in/meter-out control: the openings of the meter-in and meter-out elements are equal, the pump is under pressure in all phases of motion, and during holding the compensator standby pressure P_{sb} is maintained. Strategy B is the mode selected by the load conditions: M1 during lifting, M2 with the unloaded pump during lowering, and unloading during holding (the load is held by the check valve). The results are shown in Fig. 5. During lifting the strategies are almost equivalent (18.2 and 17.7 kJ): the equality of the openings creates an additional back pressure of 0.28 MPa in strategy A. The difference arises during lowering (4.3 against 1.2 kJ), where in strategy A the pump supplies the working fluid under pressure into the rod-side chamber, the filling of which could be provided by the make-up flow, and during holding (7.3 against 4.4 kJ). Over the cycle, 29.8 kJ is consumed with strategy A and 23.2 kJ with strategy B: mode switching reduces the energy consumed by 22 %, and the cycle efficiency at a useful work of 12.0 kJ increases from 0.40 to 0.52. This result is conservative: at the standby pressure of 1.5 MPa typical of load-sensing systems [30], the saving reaches 48 %.

A generalisation of the calculations on a grid of 81 × 141 points in the coordinates (m, v^*) is shown in Fig. 6. Under a resistive load (Fig. 6, a) the region of admissible modes is bounded from above by the pump flow rate, $v^* \le 0.182$ m/s, and inside it M1 is optimal in terms of $\Sigma\Delta p$ at any mass, while the mass affects only the efficiency (isolines η = 0.3…0.7).

Under an overrunning load (Fig. 6, b) M1 is inadmissible everywhere because of cavitation, M4 is unsuitable, and the region is bounded from above by the capacity of the make-up path, $v^* \le 0.243$ m/s. M2 is optimal almost over the whole region, while M3 is needed in the wedge of small masses and high velocities bounded by the curve $A_{out} = 0.8 \cdot A_{max}$ (see Fig. 4, d). The $\Sigma\Delta p$ isolines for M2 show that during lowering the pressure drop is determined by the mass and is almost independent of the velocity.

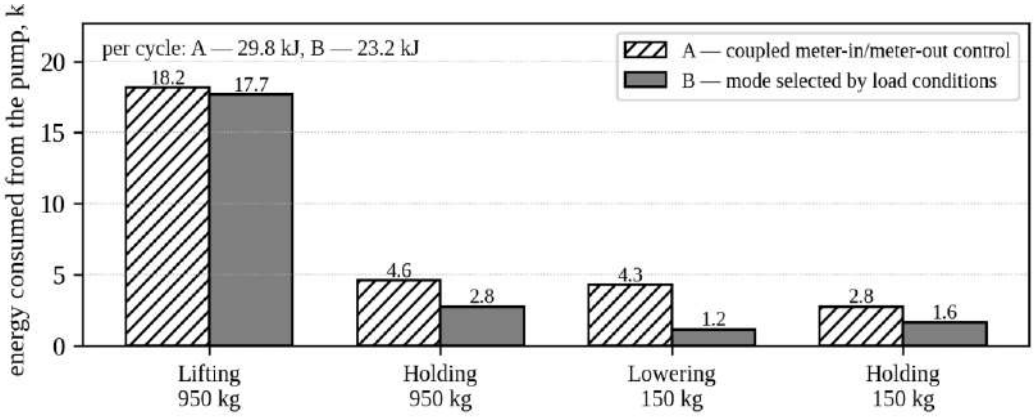


Fig. 5. Energy consumed from the pump by phases of the conventional loader cycle for the two control strategies

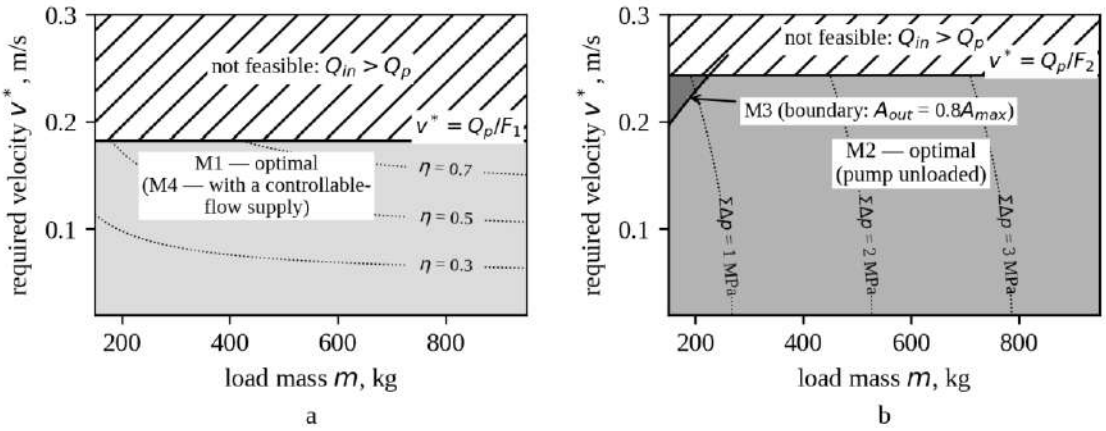


Fig. 6. Map of control modes in the coordinates "load mass — required velocity" under resistive (a) and overrunning (b) loads; hatching – infeasible combinations; at $s = -1$, M1 is inadmissible because of cavitation and M4 is unsuitable

Thus, the most influential parameters for the choice of the control mode are the sign of the load force, the ratio of the required flow rate to the supply flow rate, and the ratio of the required opening of the meter-out element to the admissible one.

Conclusions.

A quasi-static model of a hydraulic drive with a two-spool valve has been built for four flow control modes with constraints on cavitation, admissible pressure, pump flow rate, minimum controllable pressure drop and opening margin of the metering element; the assumptions and the solution procedure have been substantiated. For the boom circuit of the PKU-0.8 loader (hydraulic cylinder 80/40 mm, NSh-32 pump), 120 combinations "mode × mass × force direction × velocity" have been calculated.

Under a resistive load the total pressure drop across the metering elements does not depend on the mass and at 0.15 m/s amounts to 0.61 MPa for M1, 0.70 MPa for M2, 1.00 MPa for M3 and 0.32 MPa for M4. M1 is optimal among the modes of control by metering elements at all masses, and M4 defines the lower limit, which is 1.9 times lower at 0.15 m/s

and 14 times lower at 0.05 m/s. The transmission efficiency with a fixed-displacement pump increases with the mass from 0.39 to 0.70. The flow-rate limits of the NSh-32 pump are 0.182 m/s for lifting and 0.243 m/s for lowering.

Under an overrunning load M1 is inadmissible over the whole range of 150…950 kg: the calculated pressure in the inlet chamber is from −0.30 to −4.42 MPa, the uncontrolled motion velocity is 0.24…0.63 m/s; M4 is unsuitable. M2 with the unloaded pump provides $\Sigma\Delta p$ = 0.66…3.74 MPa at a power consumed from the pump of 0.28 kW. M3 increases $\Sigma\Delta p$ by 1.2…2.0 times and the power to 0.92 kW; therefore it is justified only for masses up to 230 kg at velocities of 0.20…0.24 m/s, where the meter-out element in M2 loses its ability to control the flow.

For the conventional loader cycle, mode switching according to the load conditions (M1 — lifting, M2 with unloading — lowering and holding) reduces the energy consumed from the pump by 22 % (from 29.8 to 23.2 kJ) in comparison with coupled meter-in/meter-out control, and the cycle efficiency increases from 0.40 to 0.52.

The mode map in the coordinates “mass — velocity” shows that the choice of the mode of a two-spool valve is determined by the sign of the load force, the ratio of the required flow rate to the supply flow rate and the ratio of the required opening of the meter-out element to the admissible one. The information of this map is the basis for choosing an appropriate method of controlling the hydraulic drive. Further work will be devoted to the dynamics of switching between the modes and to the implementation of the mode map in the form of a neural-network approximator with verification on the test bench [28].

References

1. Козлов Л. Г., Лозінський Д. О. Гідропривід з пропорційним електрогідравлічним управлінням : пат. 41887 Україна : МПК F15B 11/00. № u200900907 ; заявл. 06.02.2009 ; опубл. 10.06.2009, Бюл. № 11. 4 с.
2. Лозінський Д. О., Козлов Л. Г., Піонткевич О. В., Кавецький О. І. Оптимізація електрогідравлічного розподільника з незалежним керуванням потоків. *Вісник машинобудування та транспорту*, 2023. № 1 (17). С. 87–91. https://doi.org/10.31649/2413-4503-2023-17-1-87-91
3. Jansson A., Palmberg J.-O. Separate Controls of Meter-in and Meter-out Orifices in Mobile Hydraulic Systems. *SAE Transactions*. 1990. 99. 377–383. https://doi.org/10.4271/901583
4. Shenouda A. Quasi-Static Hydraulic Control Systems and Energy Savings Potential Using Independent Metering Four-Valve Assembly Configuration : PhD thesis. Atlanta : Georgia Institute of Technology, 2006
5. Shenouda A., Book W. Optimal Mode Switching for a Hydraulic Actuator Controlled with Four-Valve Independent Metering Configuration. *International Journal of Fluid Power*, 2008. 9 (1). 35–43. https://doi.org/10.1080/14399776.2008.10781295
6. Tabor K. A. Optimal Velocity Control and Cavitation Prevention of a Hydraulic Actuator Using Four Valve Independent Metering. *SAE Technical Paper*, 2005. 2005-01-3620
7. Pfaff J. L., Tabor K. A. Method of Selecting a Hydraulic Metering Mode for a Function of a Velocity Based Control System : US Patent 6,880,332 B2 ; assignee HUSCO International, Inc. 2005
8. Eriksson B., Palmberg J.-O. Individual metering fluid power systems: challenges and opportunities. *Proceedings of the Institution of Mechanical Engineers, Part I: Journal of Systems and Control Engineering*, 2011. 225 (2). 196–211. https://doi.org/10.1243/09596518JSCE1111
9. Liu S., Yao B. Coordinate Control of Energy Saving Programmable Valves. *IEEE Transactions on Control Systems Technology*, 2008. 16 (1). 34–45. https://doi.org/10.1109/TCST.2007.903073
10. Xu B., Ding R., Zhang J., Cheng M., Sun T. Pump/valves coordinate control of the independent metering system for mobile machinery. *Automation in Construction*, 2015. 57. 98–111. https://doi.org/10.1016/j.autcon.2015.04.012
11. Ding R., Xu B., Zhang J., Cheng M. Bumpless mode switch of independent metering fluid power system for mobile machinery. *Automation in Construction*, 2016. 68. 52–64. https://doi.org/10.1016/j.autcon.2016.04.006

12. Ding R., Xu B., Zhang J., Cheng M. Self-tuning pressure-feedback control by pole placement for vibration reduction of excavator with independent metering fluid power system. *Mechanical Systems and Signal Processing*, 2017. 92. 86–106. https://doi.org/10.1016/j.ymssp.2017.01.012

13. Cheng M., Zhang J., Xu B., Ding R. An electrohydraulic load sensing system based on flow/pressure switched control for mobile machinery. *ISA Transactions*, 2020. Vol. 96. P. 367–375. https://doi.org/10.1016/j.isatra.2019.06.018

14. Abuowda K., Okhotnikov I., Noroozi S., Godfrey P., Dupac M. A review of electrohydraulic independent metering technology. *ISA Transactions*, 2020. 98. 364–381. https://doi.org/10.1016/j.isatra.2019.08.057

15. Nguyen T. H., Do T. C., Ahn K. K. Independent Metering Valve: A Review of Advances in Hydraulic Machinery. *Journal of Drive and Control*, 2020. 17 (4). 54–71. https://doi.org/10.7839/ksfc.2020.17.4.054

16. Liu W., Li Y., Li D. Review on Inlet/Outlet Oil Coordinated Control for Electro-Hydraulic Power Mechanism under Sustained Negative Load. *Applied Sciences*, 2018. 8 (6). 886. https://doi.org/10.3390/app8060886

17. Weber J. Independent metering systems. *International Journal of Hydromechatronics*, 2018. (1). 91–106. https://doi.org/10.1504/IJHM.2018.090307

18. Lübbert J., Sitte A., Weber J. Pressure compensator control – a novel independent metering architecture. *Proceedings of the 10th International Fluid Power Conference*, 2016. 231–245

19. Kolks G., Weber J. Modiciency – Efficient industrial hydraulic drives through independent metering using optimal operating modes. *Proceedings of the 10th International Fluid Power Conference*, 2016. 1. 105–120

20. Xu B., Cheng M. Motion control of multi-actuator hydraulic systems for mobile machineries: Recent advancements and future trends. Frontiers of Mechanical Engineering? 2018. Vol. 13, No. 2. P. 151–166. https://doi.org/10.1007/s11465-018-0470-5

21. Ding R., Zhang J., Xu B., Cheng M. Programmable hydraulic control technique in construction machinery: Status, challenges and countermeasures. *Automation in Construction*, 2018. 95. 172–192. https://doi.org/10.1016/j.autcon.2018.08.001

22. Ding R., Zhang J., Xu B., Cheng M., Pan M. Energy efficiency improvement of heavy-load mobile hydraulic manipulator with electronically tunable operating modes. Energy Conversion and Management. 2019. Vol. 188. P. 447–461. https://doi.org/10.1016/j.enconman.2019.03.023

23. Lyu L., Chen Z., Yao B. Development of pump and valves combined hydraulic system for both high tracking precision and high energy efficiency. *IEEE Transactions on Industrial Electronics*, 2019. 66 (9). 7189–7198. https://doi.org/10.1109/TIE.2018.2875666

24. Vukovic M., Leifeld R., Murrenhoff H. Reducing fuel consumption in hydraulic excavators – A comprehensive analysis. *Energies*, 2017. 10 (5). 687. https://doi.org/10.3390/en10050687

25. Козлов Л. Г. Наукові основи розробки систем гідроприводів маніпуляторів з адаптивними регуляторами на основі нейромереж для мобільних робочих машин : дис. ... д-ра техн. наук : 05.02.02. Київ : НТУУ «КПІ», 2015. 421 с.

26. Піонткевич О. В. Підвищення ефективності багаторежимного гідроприводу фронтального навантажувача : дис. ... канд. техн. наук : 05.02.02. Київ, 2019. 249 с.

27. Лозінський Д. О., Піонткевич О. В., Сиротін О. А. Інноваційні підходи до підвищення енергоефективності електрогідравлічних систем. *Наукові праці Вінницького національного технічного університету*, 2025. № 2. https://doi.org/10.31649/2307-5376-2025-2-214-221

28. Лозінський Д. О., Сиротін О. А. Експериментальний стенд для дослідження характеристик електрогідравлічних систем для роботи з пасивним навантаженням. *Наукові праці Вінницького національного технічного університету*, 2025. № 4. https://doi.org/10.31649/2307-5376-2025-4-164-171

29. Lozinskyi D., Piontkevych O., Serdiuk O. Investigation of dynamic characteristics of a hydraulic drive for loading and unloading machines. International Journal of Mechatronics and Applied Mechanics. 2026. Issue 25, Vol. II. P. 39–49. https://doi.org/10.17683/ijomam/issue25/v2.4

Дата першого надходження статті до видання 11.09.2026
Дата прийняття статті до друку після рецензування 15.10.2026
Дата публікації (оприлюднення) статті 04.11.2026
Стаття поширюється на умовах ліцензії відкритого доступу(CC BY 4.0)

РЕЖИМИ КЕРУВАННЯ В ГІДРОПРИВОДІ З НЕЗАЛЕЖНИМ КЕРУВАННЯМ ПОТОКАМИ ПРИ РІЗНИХ УМОВАХ НАВАНТАЖЕННЯ

О. А. Сиротін[1], Д. О. Лозінський[1]
[1] *Вінницький національний технічний університет*

Анотація

Розглянуто гідропривод мобільної машини з пасивним навантаженням, побудований на пропорційних розподільчих елементах, які незалежно керують потоками робочої рідини на вході та виході гідроциліндра, і керованих зворотних клапанах, що забезпечують герметичність його робочих камер. Показано, що при зміні маси вантажу, знака сили навантаження відносно швидкості та заданої швидкості штока така структура потребує вибору режиму керування — призначення регулювального і повністю відкритого розподільчих елементів та стану джерела живлення. Виділено чотири режими: керування на вході, керування на виході з розвантаженням насоса, комбіноване керування і керування подачею насоса. Обґрунтовано квазістатичну постановку задачі, сформульовано припущення і складено систему рівнянь сталого режиму, яка містить рівняння рівноваги сил на поршні, рівняння витрат через розподільчі елементи та обмеження за кавітацією, допустимим тиском, подачею насоса і керованістю регулювального елемента. Критерієм порівняння режимів прийнято сумарний перепад тиску на регулювальних елементах, додатковими показниками — потужність, спожиту від насоса, і ККД передачі. На прикладі стрілового контуру фронтального навантажувача виконано розрахунок для діапазону мас вантажу, обох знаків сили навантаження і кількох заданих швидкостей, виділено недопустимі поєднання умов та їх причини. Побудовано карту режимів у координатах «маса вантажу — задана швидкість» для зустрічного і попутного навантаження; встановлено, що межі областей оптимальності визначаються знаком сили навантаження, відношенням заданої витрати до подачі джерела і потрібним відкриттям вихідного розподільчого елемента. На умовному робочому циклі навантажувача проаналізовано зменшення енергії, спожитої від насоса, при перемиканні режимів за умовами навантаження порівняно зі спільним керуванням входом і виходом. Результати призначені для синтезу алгоритмів керування гідроприводами мобільних машин з незалежним керуванням потоками.

Ключові слова: пропорційний розподільчий елемент, керований зворотний клапан, квазістатична модель, сумарний перепад тиску, кавітація, фронтальний навантажувач, розвантаження насоса, енергоефективність.